DELPHI Collaboration DELPHI 2002-071-CONF-605
21 July, 2002

A Study of the Lepton Spectrum Moments in $b \to X_c \ell \bar{\nu}$ Decays with the DELPHI Detector at LEP

M. Battaglia
CERN, Geneva (Switzerland)
M. Calvi
Universita' degli Studi di Milano-Bicocca
and I.N.F.N. Sezione di Milano (Italy)
L. Salmi
HIP, Helsinki (Finland)

Abstract

The preliminary results of a determination of the lepton energy spectrum moments, based on a sample of B s.l. decays selected from $Z^0 \to b\bar{b}$ events recorded with the DELPHI detector at LEP, are presented.

These results are interpreted in terms of constraints on the quark masses m_b and m_c and on the b-quark kinetic energy value μ_π^2. The consistency with other determinations is discussed.

Contributed paper to the 31^{st} Int. Conf. on High Energy Physics ICHEP-2002,
Amsterdam, 24-31 July 2002

1 Introduction

The extraction of the b quark couplings from semi-leptonic (s.l.) decays relies on the accurate knowledge of the quark masses and of the b-quark kinematics inside the heavy hadron. In particular, determining the $|V_{ub}|$ and $|V_{cb}|$ elements in the CKM mixing matrix with small and well understood errors, requires not only to precisely know these values but also to test the consistency of Heavy Quark Expansion predictions for inclusive s.l. B decays.

The determination of moments of the lepton energy spectrum in the $B \to X_c \ell \bar{\nu}$ B decays provides important constraints to these parameters. The consistency with the bounds set by moments of other distributions and with other data can be used to test the underlying theory assumptions.

A preliminary measurement of these moments was first reported by the CLEO Collaboration [1], but the interpretation of the results remained controversial. More recently a re-analysis of the CLEO data, but comparing the first moments of the hadronic mass in $B \to X_c \ell \bar{\nu}$ and of the photon energy in $B \to X_s \gamma$ has been published [2].

All these measurements have been performed at the $\Upsilon(4S)$ resonance. While there are obvious advantages in measuring the energy spectra in events where the decaying B rest frame almost coincides with the laboratory frame, low energy particles cannot be identified there. It is thus necessary to rely on models for extrapolating the lepton energy spectrum to zero energy or to resort to computations for a truncated spectrum. Performing this analysis at energies around the Z^0 peak allows to gain sensitivity to the full lepton spectrum, thus reducing modelling assumptions. The main challenge put by the higher energy is the accurate determination of the B rest frame.

This notes reports the preliminary results of an analysis performed on the data recorded with the DELPHI detector at LEP.

2 Data Analysis

This study is based on the analysis of s.l. B decays selected from a sample of 2.1 M $e^+e^- \to Z^0 \to q\bar{q}$ events collected with the DELPHI detector in 1994 and 1995. A sample of simulated events equivalent to about 4.5 times the data has been used to study the backgrounds. The signal selection and the energy resolution have been extracted from simulated $Z^0 \to b\bar{b}$ events containing at least one s.l. decay.

$Z^0 \to b\bar{b}$ events have been selected using a b-tagging technique based on the reconstructed impact parameter of particle tracks. In order to select the signal $b \to X_c \ell \bar{\nu}$ decays, events have been required to contain one tagged lepton candidate with momentum $p > 2.5$ GeV. These criteria selected 250 k events in the data.

2.1 Muon identification

Muons have been identified based on the response of the Muon Chambers. Details can be found in [3]. Muon candidates have been accepted if their momenta exceeded 2.5 GeV. To exclude regions with poor geometrical acceptance, only those contained within the θ_μ polar angle intervals: $|\cos\theta_\mu| < 0.62$ or $0.68 < |\cos\theta_\mu| < 0.94$, defining the barrel and the forward regions, have been retained.

Table 1: *The ratio between values measured in real and simulated events for electron identification efficiency and probability of tagging a hadron as an electron*

	1992	1993	1994	1995
Efficiency (data/MC)	0.83±0.02	0.83±0.02	0.92±0.02	0.93±0.02
Misid. Prob. (data/MC) (%)	0.57±0.04	0.77±0.05	0.76±0.05	0.70±0.06

The muon identification efficiency was measured in $Z \to \mu^+\mu^-$ events, in the decays $\tau \to \mu$ and in two-photon $\gamma\gamma \to \mu^+\mu^-$. A mean efficiency of 0.82 ± 0.01 was found with little dependence on the muon momentum and on the track polar angle. Predictions from the simulation agree, both in absolute value and in the momentum dependence, within a precision of 2%.

An estimate of the mis-identification probability was obtained by means of anti-b tagged events. After subtracting the expected remaining muon content in this sample, the misidentification probability was found to be (0.52±0.03)% in the barrel and (0.36±0.06)% in the forward regions respectively. Applying the same procedure to the simulation gave however values lower by factors of 2.03 ± 0.12 in the barrel and of 1.22 ± 0.20 in the forward regions respectively. Simulation predictions was therefore corrected by these factors.

2.2 Electron identification

Charged particles with momenta greater than 3 GeV/c and within the $0.03 < |\cos\theta_e| < 0.72$) polar angle fiducial acceptance region of the HPC e.m. calorimeter, were tagged as electron candidates based on the combination of the response of the HPC, the specific ionization dE/dx in the TPC and the RICH Cherenkov detector [4]. A momentum dependent cut was defined which provides 65% efficiency, constant over the full momentum range.

The electron identification efficiency was measured on the data by means of a sample of isolated electrons extracted from selected Compton events and a sample of electrons produced from photon conversions in the detector. The ratio between the values of the efficiencies measured in real and simulated events was parameterized as function of the transverse momentum and the polar angle of the track. Results are summarised in Table 1 . A corresponding correction factor was then applied to the sample of electrons in simulated $q\bar{q}$ events.

The probability of tagging an hadron as an electron was also measured in the data by selecting a background sample by means of the anti b-tag technique in the same manner as for muons.

To reduce the contamination from photon conversions, electron candidates were removed if they came from a secondary vertex and carried no transverse momentum relative to the direction from the primary to this secondary vertex.

The measured misidentification probability in data and the ratio with that in simulated events are given in Table 1.

2.3 Decay Reconstruction

Selected events have been divided into two hemispheres using the thrust axis. The secondary hadronic system accompanying the lepton in the s.l. decay has been reconstructed using an iterative procedure applied to the particles belonging to the same hemisphere as the tagged lepton.

Particles with $p > 1$ GeV, at least two associated hits in the vertex detector and belonging to the same hemisphere of the candidate lepton have been considered. These have been sorted in decreasing order of their probability of being B decay products based on their impact parameter significance, distance of crossing of the particle track with the jet axis w.r.t. the event primary vertex and momentum ordering. They have been iteratively tested for forming a secondary vertex. The procedure has been iterated while the following conditions have been fulfilled: invariant mass below 2.9 GeV, distance from the primary vertex exceeding 2.8 times the uncertainty and fit probability exceeding 10^{-5}. After a seed vertex has been found, charged particles with $p > 0.7$ GeV have also been tested for compatibility.

In those cases where no secondary vertex was found, single particles have been accepted when fulfilling one of the following criteria, in decreasing order of quality: a charged particle with $p > 1$ GeV having a crossing point with the jet axis significantly downstream from the primary vertex, the charged particle with $p > 1$ GeV having the largest impact parameter with positive sign using the lifetime convention, the leading particle with $p > 5$ GeV.

After this stage, identified K_s^0s and π^0s emitted within a cone of ± 0.4 rad from the lepton direction have been tested for association based on their energy, rapidity and contribution to the vertex mass.

For each decay, the energy of the B hadron was estimated as the energy sum of the identified lepton, the secondary hadronic system and the neutrino energy. The neutrino energy was computed from the missing energy in the hemisphere corrected by a function of the $E_{X\ell}$ energy determined from the simulation [5]. Neutrino energies in the range of 1.5 GeV $< E_\nu <$ 25 GeV and a minimum B energy of 25 GeV were required. The resolution of the neutrino energy was estimated to be 3.6 GeV in $B \to X\ell\bar{\nu}$ decays. The resulting resolution of the B energy was studied on simulation and found to be 11% for 80% of all inclusive semileptonic B decays and 15% for the remaining decays. Results are shown in Figure 1.

The B hadron direction has been estimated using both the momentum vector of the reconstructed $X\ell\bar{\nu}$ system and the B decay flight reconstructed by the positions of the vertex formed by the lepton with the identified charm charged decay products. An estimator, which combines these two independent measurements according to their expected resolutions as a function of the reconstructed energies and the decay distance respectively, has been defined. Resolutions of $\pm 23(17)$ mrad have been achieved in ϕ (θ).

The identified lepton was then boosted back to the reconstructed B rest frame and its energy E_ℓ^* recomputed in this frame. This resulted in a average resolution of 250 MeV on E_ℓ^* (see Figure 1).

In the reduction of the $b \to c \to \ell$ and other backgrounds it is essentially to avoid biases of the lepton energy spectrum. The separation was therefore performed using two discriminating variables, one based on the topology of the event and the other on charge correlations between the lepton and the other particles in the event. Neither of these

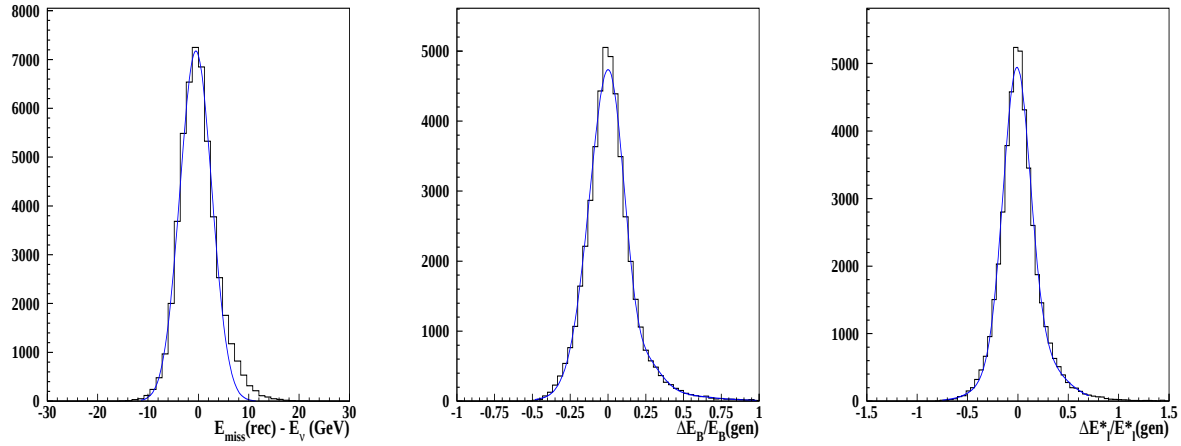

Figure 1: *The resolution on the missing energy (left), the fractional resolution on the reconstructed B hadron energy (center) and fractional resolution on the E^*_ℓ energy (right) estimated with simulation for signal $B \to X_c \ell \bar{\nu}$ events.*

Table 2: *Number of events and signal purity at different stages of the data analysis*

Cut	Data	Simulation	Signal Purity
b-Tag	247526	238870	-
Lepton id.	115820	11425	-
Sec. Vtx Reconstruction	33422	33208	59%
Signal Discriminator	18316	17972	74%

variables nor their combination is sensitive to the lepton energy, as shown in Figure 3.

The topological variable uses information on the lepton impact parameter with respect to the reconstructed secondary vertex, the topology of the tracks other than the lepton in the hemisphere as well as the direction of the lepton in the rest frame of the vertex.

The charge variable consists of a probability built from the correlation of the charge of the lepton and those of the reconstructed secondary vertex, of other vertices in the same and opposite hemispheres, of the leading fragmentation particle in the same hemisphere and of the leading kaon candidates in both hemispheres. Two-dimensional distributions are shown in Figure 2.

The final separation variable (VSep) is then obtained from the two-dimensional distribution of the topological and charge correlation variables. Lepton spectra have been selected for samples enriched and depleted by selecting on VSep (see Figure 4.) This procedure also allows to extract the shape of the backgrounds directly from the data.

The number of events and signal purity at different stages of the data analysis is reported in Table 2.

The original lepton spectrum has been extracted from the reconstructed distribution by a spectrum reweighting technique. This consisted in determining the resolution matrix relating the generated to the reconstructed spectrum for simulated signal events. Using

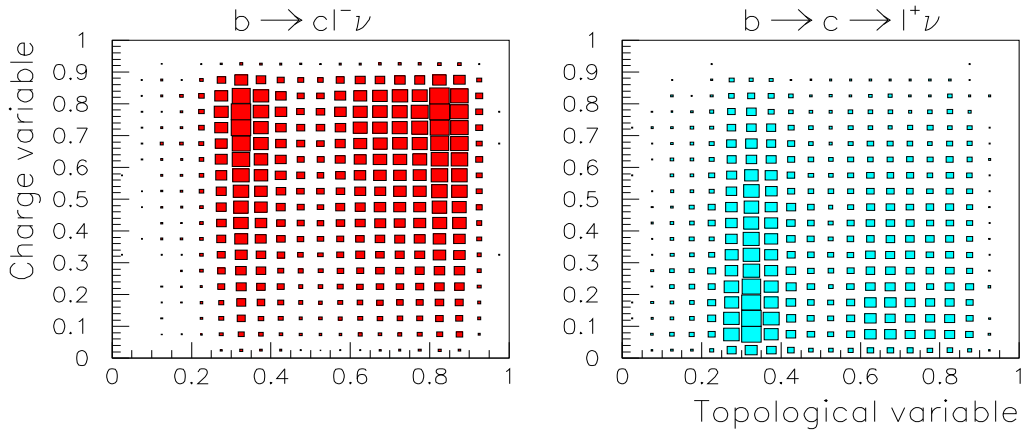

Figure 2: *Two-dimensional distribution of the topological and charge correlation variables for the signal $B \to X_c \ell \bar{\nu}$ (left) and the main background $B \to c \to X \ell \nu$ (right).*

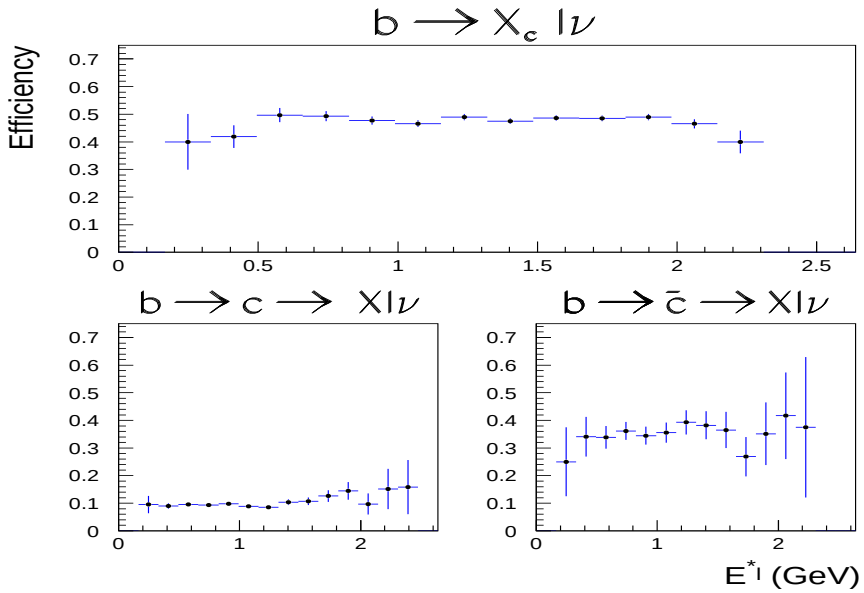

Figure 3: *The efficiencies for tagging signal $B \to X_c \ell \bar{\nu}$ (upper) and background $B \to c \to X \ell \nu$ (lower left), $B \to \bar{c} \to X \ell \nu$ (lower right) after a cut on the response of the separation variable as a function of the lepton energy E^*_ℓ.*

this matrix, the coefficients of a reweighting function for the generated spectrum have been fitted to minimise the χ^2 between the resulting spectrum and that observed in the data. The efficiency correction has been taken into account at this stage. A study of the distortions induced on the parton-level lepton spectrum by variations of the b-quark

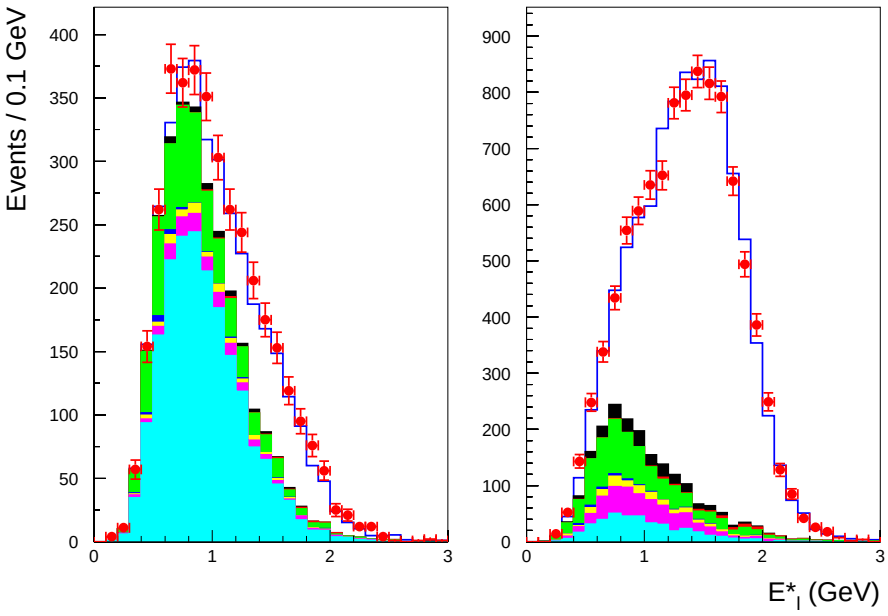

Figure 4: *The resulting E_ℓ^* spectrum for samples depleted (left) and enriched (right) in $B \to X_c \ell \bar{\nu}$ decays using the separating variable. The different sources highlighted are $b \to c \to \ell$, $b \to \bar{c} \to \ell$, $c \to \ell$, other lepton sources, misidentified hadrons, decays in flight and converted photons from bottom to top.*

Table 3: DELPHI *Preliminary Results*

$< E_\ell^* >$	(1.383±0.012) GeV
$< (E_\ell^* - < E_\ell^* >)^2 >$	(0.192±0.005) GeV^2
$< (E_\ell^* - < E_\ell^* >)^3 >$	(-0.029±0.005) GeV^3

mass m_b and kinetic term μ_π^2 has shown that a ratio of polynomials represents a suitable re-weight function. The procedure has been carefully tested on lepton spectra generated for different values of the m_b and μ_π^2 parameters and smeared according to the resolution matrix.

A regularized unfolding method [6] has also been applied as a cross-check, but the reweighting method has been preferred for its simplicity.

3 Results and Discussion

The resulting lepton spectrum is shown in Figure 5. The first, second and third moments have been computed. In order to reduce the systematic uncertainties, the second and third moments have been computed w.r.t. the average value.

In order to relate the measured moments to those computed for a B meson, some

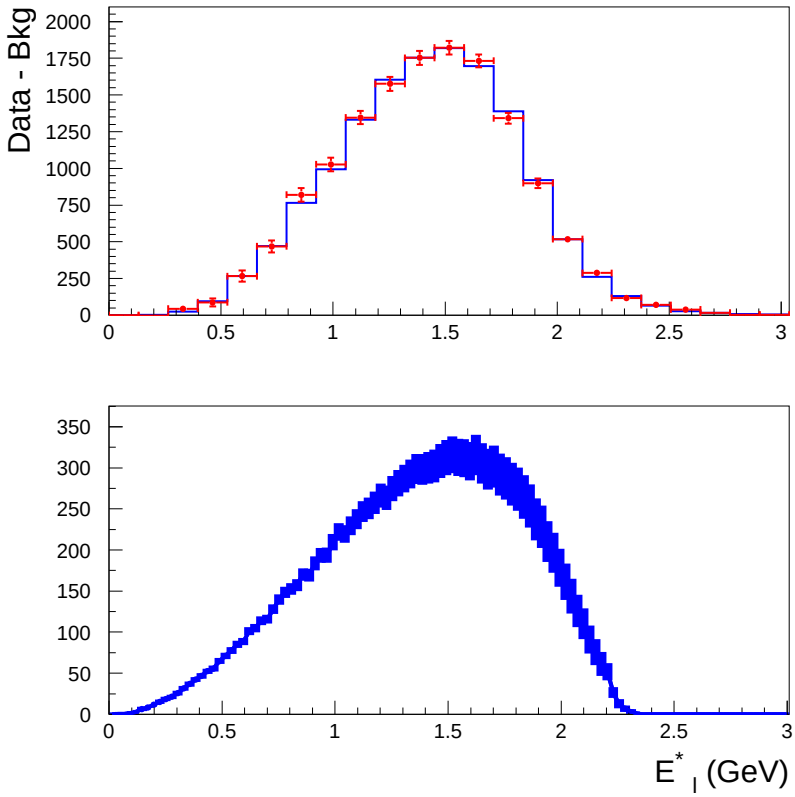

Figure 5: *The background subtracted E_ℓ^* spectrum (upper) for the selected signal sample and the unfolded lepton energy spectrum (lower). Errors per bin are shown as a band.*

corrections need to be applied. Firstly the effect of radiation needs to be corrected for. This was done using correction factors computed separately for electrons and muons following ref. [7]. Since $e^+e^- \to b\bar{b}$ events at LEP result in the production of an admixture of b-hadron species, a correction factor accounting for the bias due to the s.l. decays of the heavier b-baryons was applied, using the fraction of B_s^0 and of b-baryon left in the selected sample according to the simulation prediction. Finally, the presence of $b \to X_u \ell \bar{\nu}$ decays results in a similar bias of the lepton spectrum towards higher energies, due to the large phase space of this decay compared to $b \to X_c \ell \bar{\nu}$. This was also corrected for. The sum of these corrections accounts for shifts of 1 MeV - 3 MeV for the three measured moments. Results are given in Table 3.

The chosen selections criteria provide with a signal purity of 74% within a sizeable data sample. The stability of the results has been checked by repeating the analysis restricting to different data subsets and by changing several cuts applied. The changes in the cuts imply a variation of the accepted statistics over a factor of three and of the signal purity over a range from 71% (Loose Vsep) up to 82% (Tight Cuts).

The results have been found to be stable within their statistical uncertainty (see Table 4). Several sources of systematic uncertainties have been investigated. The main

Table 4: *Summary of the systematic checks*

Selection	Nb. of Events	$< E_\ell >$ (GeV)	$< (E- < E_\ell >)^2 >$ (GeV^2)	$< (E- < E_\ell >)^3 >$ (GeV^3)
Standard	18316	1.383±0.012	0.192±0.005	-0.029±0.006
e only	7559	1.384±0.019	0.188±0.008	-0.031±0.009
μ only	10757	1.382±0.016	0.195±0.007	-0.028±0.008
Loose Vsep	21901	1.380±0.011	0.195±0.005	-0.030±0.005
Tight Vsep	11266	1.383±0.015	0.195±0.006	-0.029±0.008
Tight b-Tag	14708	1.385±0.013	0.189±0.006	-0.030±0.007
Tight Cuts	10128	1.382±0.016	0.195±0.007	-0.029±0.008

Table 5: *Summary of the sources of systematic uncertainties*

Source	Range	$\delta < E_\ell >$	$\delta < (E- < E_\ell >)^2 >$	$\delta < (E- < E_\ell >)^3 >$
$< X_E^b >$	0.702±.008	±0.0026	±0.0003	±0.0007
B species	PDG2002	±0.0020	±0.0010	±0.0005
$B \to D, D^*, D^{**}\ell\bar{\nu}$	±13%/5%/25%	±0.0060	±0.0030	±0.0046
E_ℓ^* Resolution		±0.0020	±0.0020	±0.0010
Bkg Subtraction		±0.0030	±0.0040	±0.0010
Unfolding		±0.0050	±0.0050	±0.0030
Total		±0.0092	±0.0075	±0.0057

sources are due to the fractions of the different D species in the decays. Other contributions are related to the B species and the background subtraction. The latter has been estimated by comparing the results using the background shape extracted from the anti-tagged data with that predicted from the simulation.

Results are summarised in Table 5.

3.1 Data Interpretation

The interest of determining the moments of distributions in s.l. B decays stems from the extraction of parameters and the possibility to test the underlying theory. These interpretations of the experimental data deals with issues which depends on the confidence in the theoretical predictions and in the control of higher order corrections which have not yet been computed. In this section we discuss the implications of the results for the lepton energy spectrum, presented here, and for the hadronic spectrum, presented in a companion paper [11]. Two different approches can be followed. The first [8] is based on an expansion on the pole masses m_b and m_c and expresses the b-energy parameter as λ_1, while the second [9] uses running heavy quark masses $m_b(\mu)$ and $m_c(\mu)$ and the kinetic energy expectation value μ_π^2, corresponding to λ_1.

The n-th moments can be related to the heavy quark running masses $m_b(\mu)$ and $m_c(\mu)$ and the μ_π^2 parameter through the following relationship, which accounts for corrections

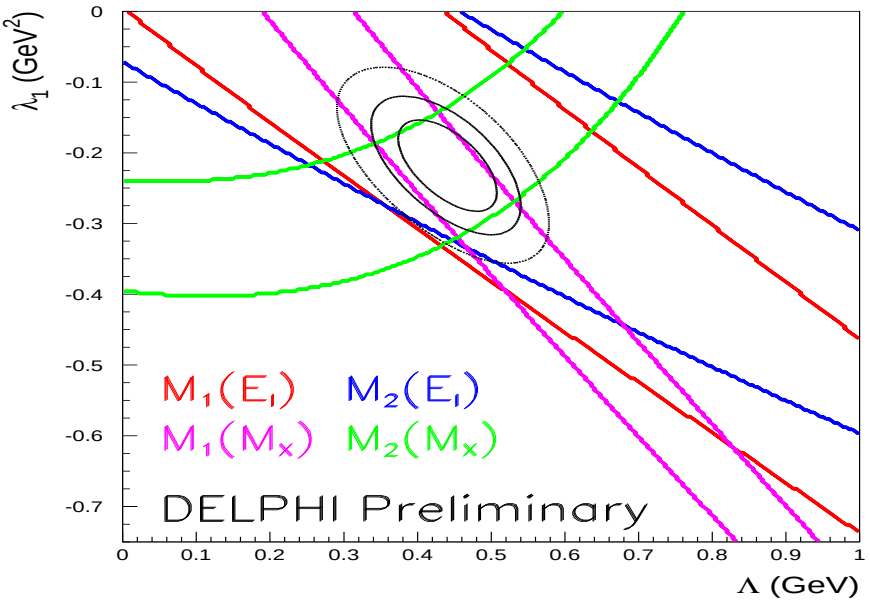

Figure 6: *The constraints on the* $\bar{\Lambda}$ - λ_1 *plane obtained from the combination of the first two moments of the lepton energy (* $M_1(E_\ell)$, $M_2(E_\ell)$ *) and hadronic mass (* $M_1(M_X)$, $M_2(M_X)$*) measured by* DELPHI. *The bands represents the regions selected by each moment within* $\pm 1\sigma_{stat+syst}$. *The ellipsis shows the* 1σ, *68% and 90% C.L. respectively.*

up to the $\beta_0\alpha_s^2$ and $1/m_b^3$ order:

$$M_n = \frac{m_b^n(\mu)}{2^n}\phi_n(r)(1+\frac{4\alpha_s}{3\pi}a_n(r,\mu)+\frac{4}{3}\beta_0\frac{\alpha_s^2}{\pi^2}a_n^{(2)}(r,\mu)+$$

$$\frac{\mu_\pi^2}{m_b^2(\mu)}b_n(r)+\frac{\mu_G^2}{m_b^2(\mu)}c_n(r)+\frac{\rho_D^3(\mu)}{m_b^3(\mu)}d_n(r)+\frac{\rho_{LS}^3(\mu)}{m_b^3(\mu)}s_n(r))$$

where $r = m_c^2(\mu)/m_b^2(\mu)$ and the ϕ_n, a_n, b_n, c_n and s_n are coefficients whose form can be found elsewhere [10].

It is convenient to express the heavy quark masses in terms of a single parameter $\bar{\Lambda}(\mu)$ by using the following mass expansion:

$$m_b(\mu) = M_B - \bar{\Lambda}(\mu) - \frac{\mu_\pi^2-\mu_G^2}{2m_b(\mu)} - \frac{\rho_D^3-\rho_{LS}^3}{4m_b^2(\mu)} - \delta_B$$

with $\delta_B \propto \frac{\Lambda_{QCD}^3}{4m_b^2}$. A similar expression holds for $m_c(\mu)$, where $\delta_D \propto \frac{\Lambda_{QCD}^3}{4m_c^2}$.

Results obtained from the measured values of the first two moments of the hadronic mass spectrum and lepton energy spectrum have been found to be compatible. An exemplification is given in Figure 6 showing constraints extracted in the $\bar{\Lambda}$ - λ_1 plane. The error bands indicate the experimental statistical and systematic uncertainties discussed above. In extracting the constraints on $\bar{\Lambda}$ and λ_1 additional systematics arise from the uncertainties in the power corrections. These have been included in this study by

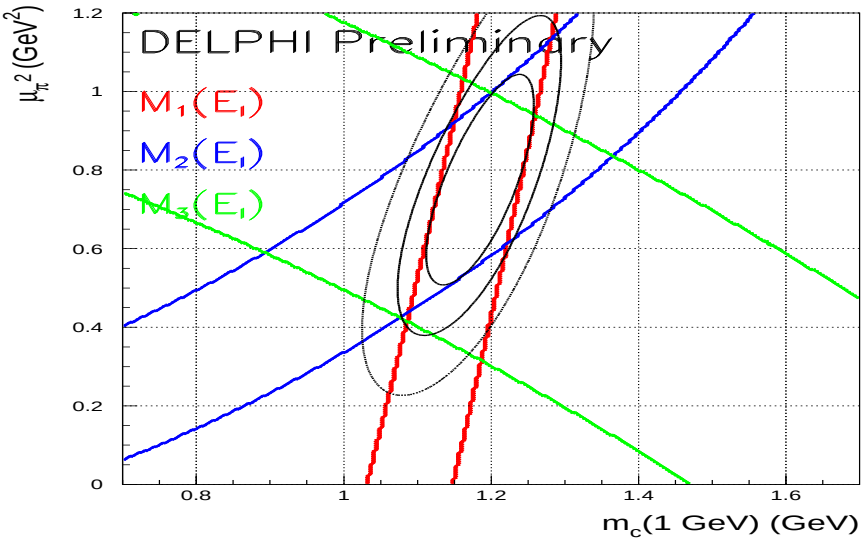

Figure 7: *The constraints on m_c plane obtained from the first two moments of the lepton energy. The bands represents the regions selected by each moment within $\pm 1\sigma_{stat+syst}$. The ellipsis shows the 1σ, 68% and 90% C.L. respectively. The band representing the third moment is also shown, although it has not been used in the fit.*

varying the coefficients of the $1/m_b^3$ expansion [8] as follow: $\rho_1 = (\frac{1}{2}0.5^3 \pm \frac{1}{2}0.5^3) GeV^3$, $\rho_2 = (0. \pm 0.5^3) GeV^3$, $\mathcal{T}_i = (0. \pm 0.5^3) GeV^3 (i = 1, 4)$ and $\alpha_s = 0.22 \pm 0.03$. The resulting constraints are:

$$\bar{\Lambda} = (\ 0.44 \pm 0.04(stat) \pm 0.05(syst) \pm 0.07(1/m_b^3 + \alpha_s))\ GeV$$

$$\lambda_1 = (-0.23 \pm 0.04(stat) \pm 0.05(syst) \pm 0.08(1/m_b^3 + \alpha_s))\ GeV^2$$

In this study also the third moment has been determined. While its interpretation in the extraction of the mass and energy parameters is not yet well established, in principle it proves useful for determining the ρ_1 (ρ_D^3) parameter which accounts for an important fraction of the $1/m_b^3$ corrections. Another way to express these results is to extract the charm quark mass m_c by using an independently determined value of m_b. In fact, while there have recently been several determinations of m_b, with different techniques and providing consistent results, the situation for m_c appears more controversial. Using the first two moments of the leption energy spectrum and m_b=4.60±0.05 GeV, with the second theoretical formulation we find (see Figure 6):

$$m_c(1\ \text{GeV}) = (1.19 \pm 0.05(stat.) \pm 0.05(syst.) \pm 0.07(m_b) \pm 0.04(1/m_b^3))\ GeV$$

where the quoted uncertainties are statistical, systematical, ± 0.050 GeV on m_b and ± 0.13 GeV^3 on the ρ_D^3 and ρ_{LS}^3 terms in the $1/m_b^3$ corrections.

4 Conclusion

A study of the moments of the lepton energy spectrum in s.l. B decays has been performed with the data collected with the DELPHI detector at LEP. The preliminary results give a determination of the first three moments as:

$$< E_\ell^* > = (1.383 \pm 0.012 \pm 0.009) \text{ GeV}$$
$$< (E_\ell^* - < E_\ell^* >)^2 > = (0.192 \pm 0.005 \pm 0.008) \text{ GeV}^2$$
$$< (E_\ell^* - < E_\ell^* >)^3 > = (-0.029 \pm 0.005 \pm 0.006) \text{ GeV}^3$$

These results are interpreted in terms of constraints on the values of the heavy quark masses and the b-quark kinetic energy.

Acknowledgements

We are greatly indebted to N.Uraltsev and P.Gambino for contributing to the theoretical predictions to be used in this paper and for helpful discussions during this work.

References

[1] J. Bartelt *et al.* (CLEO Collaboration), CLEO-CONF 98-21.

[2] D. Cronin-Hennessy *et al.* (CLEO Collaboration), Phys. Rev. Lett. **87** (2001)251808

[3] G.R. Wilkinson, *Improvements to the Muon Identification in the 94C2 Short DST Production* DELPHI 97-37 PHYS 690.

[4] C. Kreuter, *Electron Identification using a Neural Network* DELPHI 96-169 PHYS 658.

[5] P. Abreu *et al.* (DELPHI Collaboration), Zeit. Phys. **C 71** (1996), 539.

[6] V. Blobel, OPAL technical Note TN361 (1996).

[7] D. Atwood and W. J. Marciano, Phys. Rev. **D 41** (1990) 1736.

[8] A. F. Falk and M. Luke, Phys. Rev. **D57** (1998)424. For the moments of the lepton energy spectra P.Gambino, private communication.

[9] M.B.Voloshin Phys. Rev. **D51** (1995)4934.
I. I. Bigi, M. A. Shifman and N. Uraltsev Ann. Rev Nucl.Part. Sci **47** (1997)591.

[10] N. Uraltsev, private communication.

[11] D. Bloch *et al.*, DELPHI 2002-070 CONF 604, contributed paper to this Conference.